J. Membrane Biol. 19, 339–355 (1974)

Studies on the Formation of a Permeable Cell Membrane Junction

II. Evolving Junctional Conductance and Junctional Insulation

S. Ito, E. Sato and W. R. Loewenstein

Department of Physiology and Biophysics,
University of Miami School of Medicine, Miami, Florida 33152, U.S.A.
and Department of Biology, Faculty of Science,
Kumamoto University, Kumamoto 860, Japan

Received 25 September 1974

Summary. Coupling by permeable membrane junction between single pairs of newt embryo cells (macroblastomeres) was induced *in vitro*. At the same time, the resistance of the developing cell-to-cell diffusion channels (junctional membrane) and that of their insulation from the exterior (junctional insulation) were determined by electrical measurement. From the moment the cell coupling was first detected electrically, the resistance of junctional membrane fell gradually to a relatively steady level during 0.5–1 hr. Meanwhile, the resistance of junctional insulation rose gradually to a peak, then declined somewhat to a relatively steady level. An upper limit for the steady-level resistivity of junctional membrane was estimated from measurements on partly separated cells coupled by 3–4 strands of 1 μ^2 cross-section; this estimate is 10^{-2} Ω cm^2, 6 orders of magnitude less than the resistivity of nonjunctional membrane. Viewed in the light of a model proposed earlier (W. R. Loewenstein, 1966), these results suggest that junctional coupling may develop by accretion of diffusion-channel units of $\leqq 10^{-2}$ Ω cm^2 resistivity.

The essential functional elements in a coupling membrane junction are the channels for cell-to-cell diffusion *(junctional membranes)* and the insulation *(junctional insulation)* that seals off the interior of the connected system from the exterior (Loewenstein, 1966) (Fig. 1). These elements are not patent or present when the cells are separate; they develop as functional entities when the cells are joined. We inquire here into the development of these entities by determining the conductances of junctional membrane and junctional insulation in the course of junction formation between newt embryo cells (macroblastomeres). These giant cells are readily induced to form junctions *in vitro* (Ito & Loewenstein, 1969); and the simple system consisting of a single joining pair of such cells reduces to a manageable number the continuous electrical measurements needed for determining the conductances of the evolving junctional membrane and junctional insulation.

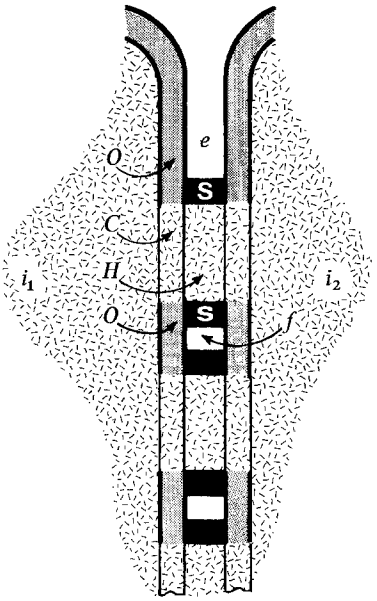

Fig. 1. Junction model. Schematic model of permeable membrane junction, based (exclusively) on measurements of conductance and fluorescent tracer diffusion. Multiple cell-to-cell passageways *(junctional units)* consisting of *junctional membrane* (*C*), highly permeable, containing the membrane diffusion channel; *nonjunctional membrane* (*O*), relatively impermeable; and *junctional insulation* (*S*), a diffusion barrier circumscribing aqueous channel (*H*). The intracellular compartment, namely the interiors of the two adjacent cells (i_1, i_2) and the cell-to-cell passageways are stipled; the extracellular compartment, *e* and *f*, is shown in white. (From Loewenstein, 1966)

Materials and Methods

Junctions were made between pairs of daughter cells of macroblastomeres isolated from *Triturus pyrrhogaster* embryos. The paired cells were of similar size. Junction formation was induced by the method of *imposed random contact*, described in the first paper of this series (Ito, Sato & Loewenstein, 1974). This paper also gives the procedures for cell isolation and junction breakage, and the composition of the medium.

Electrical Measurements

The basic measurement consisted of determinations of membrane voltage attenuation and of nonjunctional membrane resistances. The electrode arrangement is illustrated in Fig. 2. In this arrangement, with three intracellular microelectrodes (current-passing, 20–30 MΩ; voltage-recording, 20–50 MΩ), the test current *i* (rectangular pulses of 300–400 msec duration) flowed between a microelectrode inside one of the cells (*I*) and the grounded exterior; and the resulting steady-state displacements (*V*) of membrane potential in the two cells, i.e., the input- (V_1) and the transfer voltage (V_2), were measured against ground during coupling development. In a variant with four microelectrodes,

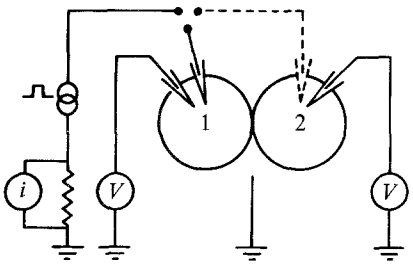

Fig. 2. Diagram of the basic measuring arrangement during coupling. Rectangular current pulses i are passed between interior of cell *1* and cell exterior, and the resulting steady-state voltages V_1, V_2 are measured between the exterior and the interiors of cells *1* and *2*. Cell exterior is grounded. In a variant, current is also injected into cell *2* with the aid of a fourth microelectrode (stipled); the current is then switched alternately into cell *1* and *2*

one current-passing microelectrode was in each cell; current was then alternately switched into cells *1* and *2*. In this way, transfer voltages could be measured in both directions across the junction and the values were averaged.

A complete measuring sequence consisted of (i) determination of membrane resistance r_{o_1} and r_{o_2} before cell contact; (ii) continuous monitoring of input and transfer resistance during junction formation; and (iii) determination of membrane resistances r_{o_1}, r_{o_2} after the breaking of the junction.

The cells were in normal (control) medium throughout the experiments, except for two cases in which the cells were in colchicine-containing (1.09 mM) medium throughout the measurements to block cell movement and division (Exp. No. 6 and 30 in Table 1).

Cell-to-Cell Resistance Measurement

An accessory measurement consisted of a determination of cell-to-cell resistance. Here, the current flowed between two microelectrodes (10–15 MΩ) placed in each cell, and the corresponding voltage was measured across the cell junction with another pair of microelectrodes (10 MΩ) connected to the grids of high-impedance amplifiers. Both the current-passing and the voltage-recording circuits were isolated from ground (Fig. 6*A*). The test current largely bypassed nonjunctional membrane once a low-resistance path had developed at the membrane junction (the resistance of this path was generally one order of magnitude lower than that of the nonjunctional path when full coupling had been established).

In either kind of measurement, the measurements were taken continuously during junction formation. r_{o_1} was measured directly with the aid of an intracellular current-passing- and an intracellular voltage-recording electrode; r_{o_2} was either measured directly or computed as

$$r_{o_2} = r_{o_1} \cdot \frac{d_1^2}{d_2^2}$$

where d_1 and d_2 are the diameters of the cells.

All experiments were done at room temperature ranging 22 to 24 °C.

Electron-microscopy

The cell pairs used for electron-microscopy were fixed by glutaraldehyde 1 hr after they had been micromanipulated into contact *(imposed random contact)*. The cells were pushed together by the electrodes but they were not impaled on them, because electrode retraction from fixed cells caused the junctions to break. The procedure was (1) to leave the cells in normal (control) medium for 60 min after contact; (2) to exchange the medium for a solution of 3% glutaraldehyde in 0.1 M phosphate buffer (pH 7.4); (3) to transfer the dish after 15 min to a refrigerator (4 °C) for a further 16-hr fixation (the cells were left untouched from (1) to (3)); (4) to rinse for 90 min in the buffer; and (5) to fix again for 90 min in 1% buffered osmium tetraoxide. Sections (in araldite) of 0.08–0.1 μ were stained with lead citrate.

Results

Junctional Membrane- and Junctional Insulation Resistance

The basic measurements (Fig. 2) were taken on single coupling pairs of cells. For such a one-junction cell system, the equivalent circuit is given, to a first approximation, by Fig. 3: $2r_c$ represents the junctional membrane resistance (the resistance of all junctional membrane elements in parallel, Fig. 1); r_s, the junctional insulation resistance; and r_{o_1} and r_{o_2}, the non-junctional membrane resistances. [1]

We induced formation of the junction by micromanipulating two separate cells into contact, allowed the cells to develop coupling, and then separated them again by micromanipulation. We determined r_{o_1} and r_{o_2} in the separate cells and measured i, V_1 and V_2 continuously during coupling. We assume constancy for r_{o_1} and r_{o_2} during coupling, because the area of nonjunctional membrane converted into junctional membrane during the coupling process amounts to a very small fraction of the nonjunctional area (*see* p. 349) and because, when r_{o_1} and r_{o_2} were determined both before cell contact and after separation, the values differed by less than 15%.

1 The resistive, but not the reactive circuit elements are represented since only steady-state currents will be considered. The cytoplasmic resistances of these large cells and the resistance of the external medium are neglected. r_c is half the junctional membrane resistance measured in the cell-to-cell direction. Strictly, besides the resistance component of the junctional membranes, r_c includes the resistance component of the possible inter-junctional membrane space circumscribed by junctional insulation and belonging to the intracellular compartment in the coupled state. r_s is understood to include, besides the resistance of junctional insulation S, a component representing the diffusion constraints in the intercellular space; the relative magnitude of this component is unknown. We should like to emphasize that the morphological equivalents of the C and S elements are unknown (*see* p. 354; and Loewenstein, 1974 for a discussion on possible structural correlates). The model of Fig. 1 represents the intra- and extracellular relationships of the two elements only in terms of their resistances to diffusion. The present electrical measurements determine the total S resistance and total C resistance to small-ion diffusion in the cell junction.

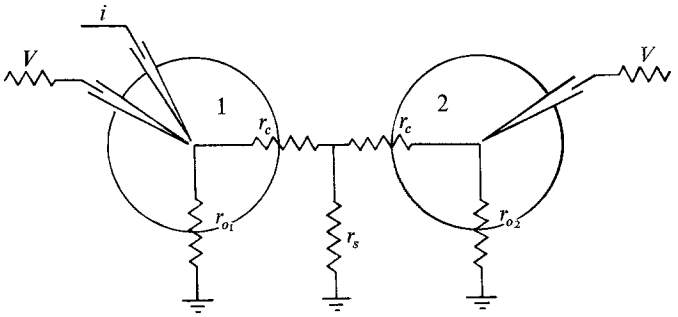

Fig. 3. Equivalent circuit of a coupling cell pair in a basic measurement. r_c, 1/2 junctional membrane resistance; r_s, junctional insulation resistance; r_{o_1}, r_{o_2}, nonjunctional membrane resistances. (The two cells *1*, *2*, which form a junction, are drawn separate here to accommodate the circuit diagram)

Thence, with the aid of Kirchoff's laws,

$$r_c = \frac{V_1 - V_2}{i - \left(\frac{V_1}{r_{o_1}} - \frac{V_2}{r_{o_2}}\right)} \tag{1}$$

and

$$r_s = \frac{V_1}{i - \left(\frac{V_1}{r_{o_1}} + \frac{V_2}{r_{o_2}}\right)} - \frac{i - \frac{V_1}{r_{o_1}}}{i - \left(\frac{V_1}{r_{o_1}} + \frac{V_2}{r_{o_2}}\right)} \cdot r_c. \tag{2}$$ [2]

Using these equations, we have computed the junctional membrane resistance $2r_c$ and the junctional insulation resistance r_s for forming cell junctions in which continuous measurements were taken during coupling development.

Fig. 4 illustrates the results of such a measurement. Shown on the same time scale are: (*A*) the original chart record; (*B*) the plot of the coupling ratios V_2/V_1; (*C*) the plot of the primary data V_1, V_2 ($i = 0.92 \times 10^{-8}$ A); and (*D*) the plot of the computed $2r_c$ and r_s. The plots begin 22 min after cell contact, the time the first transfer voltage V_2 became detectable (coupling onset). At this time, the junctional membrane resistance $2r_c$ was about 20×10^6 Ω. It then fell 33-fold over the following 30 min of coupling development, reaching a relatively steady level of 0.6×10^6 Ω about 52 min after cell contact. Meanwhile, the junctional insulation resistance r_s rose from 0.8×10^6 Ω to a peak of 8×10^6 Ω, then settled at a relatively steady level of about 4×10^6 Ω.

2 The equations have been written for the case of a single current source in cell *1*, where the input voltage is V_1 and the transfer voltage V_2. For the measurement variant with an additional current source in cell *2*, the input and transfer voltages are, respectively, V_2 and V_1; and in the equations, the subscripts 1 and 2 are interchanged throughout.

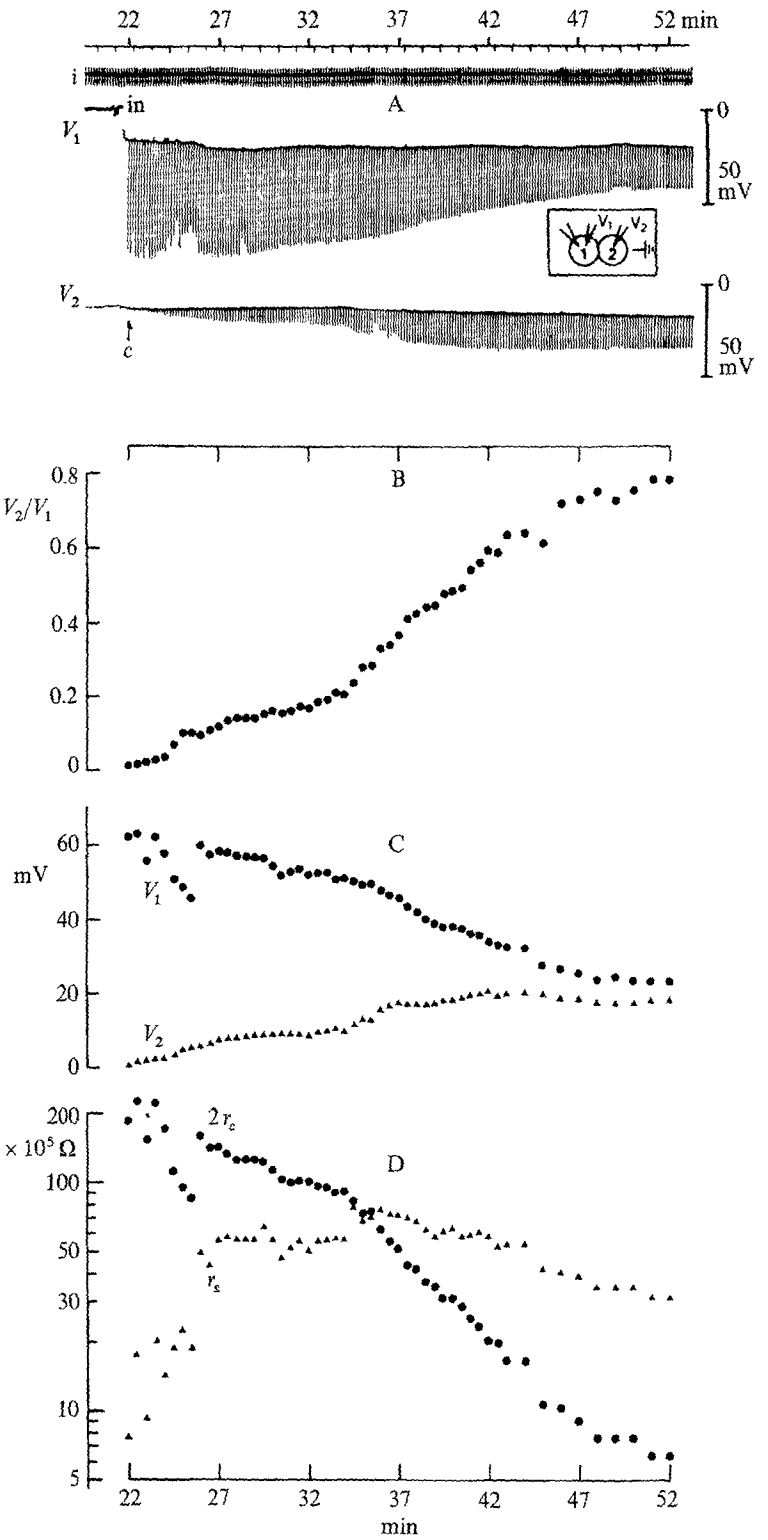
22
27
32
37
42
47
52 min
i
in
A
V_1
0
50 mV
V_2
c
B
V_2/V_1
0.8
0.6
0.4
0.2
0
C
mV
60
40
20
0
D
$2r_c$
r_s
$\times 10^5\ \Omega$
200
100
50
30
10
5
min

Fig. 4

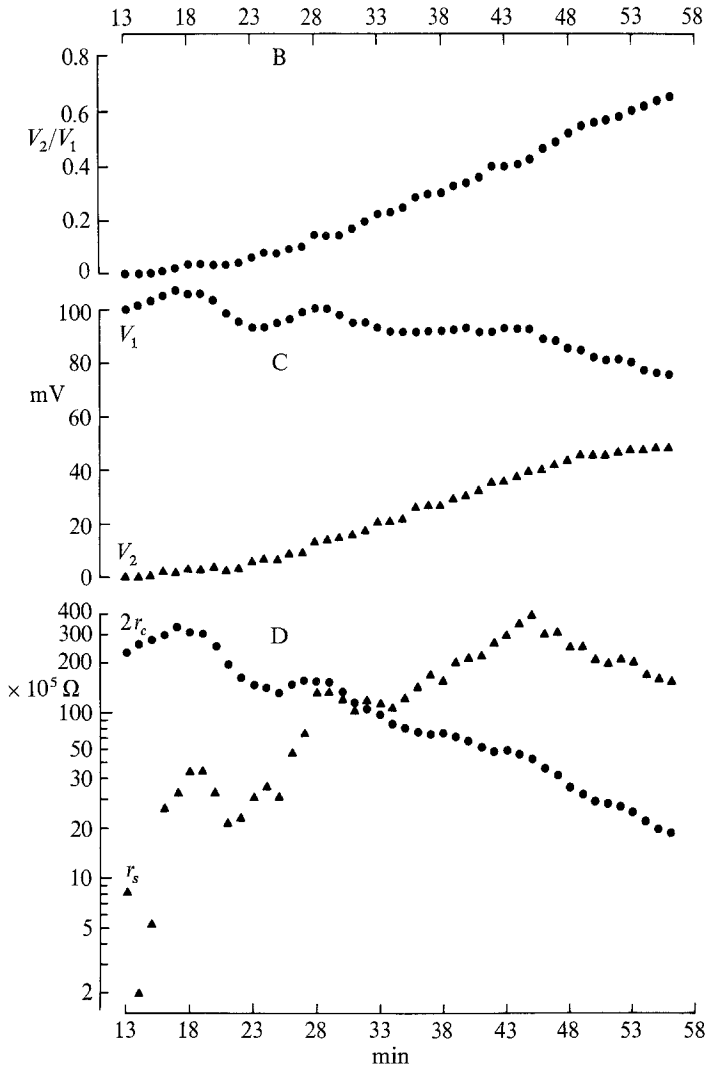

Fig. 5

Fig. 4. Junctional membrane and insulation resistances. (*A*) Chart record of a continuous measurement during junction formation. *i*, current square pulses, 300 msec duration; *V*, changes in membrane potential. Zero points on right-hand calibrations mark the membrane potentials at 0 current. The V_2-microelectrode was inside the cell since the establishment of cell contact *(random imposed contact)*; the V_1-microelectrode was inserted when V_2 became detectable (*c* mark). Cell diameters: *1*, 400 μ; *2*, 325 μ. (*B*) Coupling ratio V_2/V_1. (*C*) Primary data: V_1 (•) and V_2 (▲); $i=0.92\times10^{-8}$ A; $r_{o_1}=9.6$ MΩ; $r_{o_2}=14.5$ MΩ. (*D*) Computed junctional membrane resistance $2r_c$ (•) and junctional insulation resistance r_s (▲); logarithmic scale. The time scale on the abscissa is common for the chart record and the plotted curves

Fig. 5. Junctional membrane and insulation resistances. (*B*) V_2/V_1. (*C*) Primary data: V_1 (•) and V_2 (▲); $i=2\times10^{-8}$ A; $r_{o_1}=5.5$ MΩ; $r_{o_2}=9.8$ MΩ; (*D*) $2r_c$ (•); r_s (▲). The cells were in colchicine-containing medium (1.09 mM) blocking cell division and movement throughout the measurement. The chart record of this experiment is shown in Fig. 17, paper I. Cell diameters: *1*, 500 μ; *2*, 375 μ

Fig. 5 gives the results of another case in which cell movement and division had been blocked by colchicine (1.09 mM). Colchicine did not seem to affect the time of coupling onset, as already noted in paper I; nor did it affect the development of a low junctional membrane resistance: r_c fell one order of magnitude during coupling in this example. The junctional insulation resistance r_s rose two orders of magnitude. The extent of this rise was more typical (even for the experiments in normal medium) than that of the experiment in Fig. 4.

Measurements of this sort were performed on 11 cell junctions. In all cases, *the development of coupling was characterized by a gradual fall in junctional membrane resistance and a gradual rise in junctional insulation resistance.* The junctional membrane resistances fell monotonically over 30–67 min after the coupling onset to a relatively steady level (0.6 – 2.5 MΩ);

Table 1. Resistances of junctional membrane ($2r_c$), junctional insulation (r_s) and nonjunctional membrane (r_{o_1}, r_{o_2})

Exp. No.	$2r_c$ (MΩ)		r_s (MΩ)			r_{o_1} (MΩ)	r_{o_2} (MΩ)	R_{o_1} (KΩcm²)
	initial[a]	final[b]	initial[a]	peak[c]	final[d]			
23	35	1.1 (48, 40)	2.0	150 (43)	65	5.6	6.7	24
29	20	2.5 (57, 45)	0.6	>500*		5.2	7.8	17
32	5	0.6 (58, 50)	0.3	16 (48)	3	3.4	3.7	24
53	2	0.6 (45, 30)	0.3	>45*		2.3	7.9	17
56	10	0.6 (53, 40)	0.4	16 (43)	4	2.4	1.3	9
27–1[f]	16	0.6 (53, 31)	0.8	8 (36)	4	9.6	14.5	48
27–2	11	1.3 (52, 28)	1.2	213 (44)	65	5.0	5.0	22
104	5	1.6 (88, 55)	1.4	>260*		6.3	8.0	40
105	6	0.97 (77, 67)	0.9	84 (69)	e′	4.4	3.3	28
6[g,h]	34	1.9 (56, 43)	0.2	40 (46)	16	5.5	9.8	43
30[h]	12	2.2 (72, 52)	0.5	89 (70)	89[e]	4.9	5.5	31
Mean[i]	14.2 ±11.3	1.3 ±0.7	0.8 ±0.6	>129 ±149	35 ±37	5.0 ±2	6.7 ±3.5	27 ±12

[a] Resistance value at the time of coupling onset.
[b] "Steady" level values. In parentheses the time (min) after cell contact and the time (min) after coupling onset (*see* footnote 3).
[c] Peak values, except cases marked * where r_s was still rising at the time of the last measurement. In parentheses the time after cell contact.
[d] "Steady" level values.
[e] r_s rose monotonically in this case.
[e′] Final value near peak but uncertain whether at "steady" level.
[f] Shown in Fig. 4.
[g] Shown in Fig. 5.
[h] Cells in 1.09 mM colchicine-containing medium, blocking cytokinesis and cleavage; all other experiments in normal medium.
[i] Mean with SD including values marked *.

the junctional insulation resistance peaked (8 – > 500 MΩ) after 14 – ~ 35 min, then levelled off, generally below peak(3 – 8 9 MΩ) after 15–40 min. Table 1 summarizes the computed resistances of junctional membrane and junctional insulation, and also gives the corresponding resistances, r_o, and specific resistance, R_{o_1}, of nonjunctional membrane.[3]

Cell-to-Cell Resistance

Given the preceding results, one would expect that a measurement of the kind diagrammed in Fig. 6*A* should show that the cell-to-cell resistance, the resistance between points p_1 and p_2 in Fig. 7, diminishes in the course of coupling. Indeed, this was confirmed. In the example of Fig. 6*B*, the first measurement was begun 15 min after contact, well after coupling onset. At this time, the cell-to-cell resistance (the V/i slope) was 2.7×10^6 Ω. It declined to about one-seventh this value over the following 65 min. This same trend was seen in the other six measurements of this kind.

It may be thought that such a measurement would be the most straightforward way for following a change in r_c. Unfortunately, the interpretation of such a measurement is complicated, because a decline in cell-to-cell resistance may reflect a fall in r_c, a fall in r_o and, unless $r_{o_1} = r_{o_2}$, a fall in r_s. While we infer from the initial and final measurements of r_o in the separate cells that both r_{o_1} and r_{o_2} remain rather constant during coupling, our only quantitative information on the time course of r_s came from the basic measurements described in the preceding section (which also gave r_c directly). Thus, the cell-to-cell resistance measurements are, at most, confirmatory of the basic ones.

Junctional and Nonjunctional Specific Membrane Resistance

Fig. 8 shows electron-micrographs of the surface of the cell system. The fixation of the cells is too poor to give useful information on junctional structure (the embryonic newt cell material does not fix well with the standard techniques). The electron-micrographs serve, however, to show two points which are of interest in connection with the determination of specific resistances (resistances of unit area) of junctional and nonjunctional membrane: (i) the nonjunctional membrane is rather unconvoluted (although there are a few motile protuberances by which the cells establish contact) (Fig. 8*a*, *b*); and (ii) the area of membrane contact between fully coupled cells is very much smaller than that of the region of cell "contact" apparent in the light microscope (Fig. 8*c*).

From the first point, it is evident that one can get good estimates of nonjunctional membrane area from measurements of the cell diameter.

3 These measurements were performed during the 1974 breeding season; those of the preceding paper, generally during the 1972/1973 seasons, except for the series marked *f'* in Table 1, paper I. The V_2/V_1 and r_c parameters were similar in all seasons. However, the times required for coupling onset and the times for plateau coupling were generally longer in the experiments of the 1974 season. Thus, in regard to the time course of coupling development, the present measurements are comparable only with the series *f'* in Table 1, paper I.

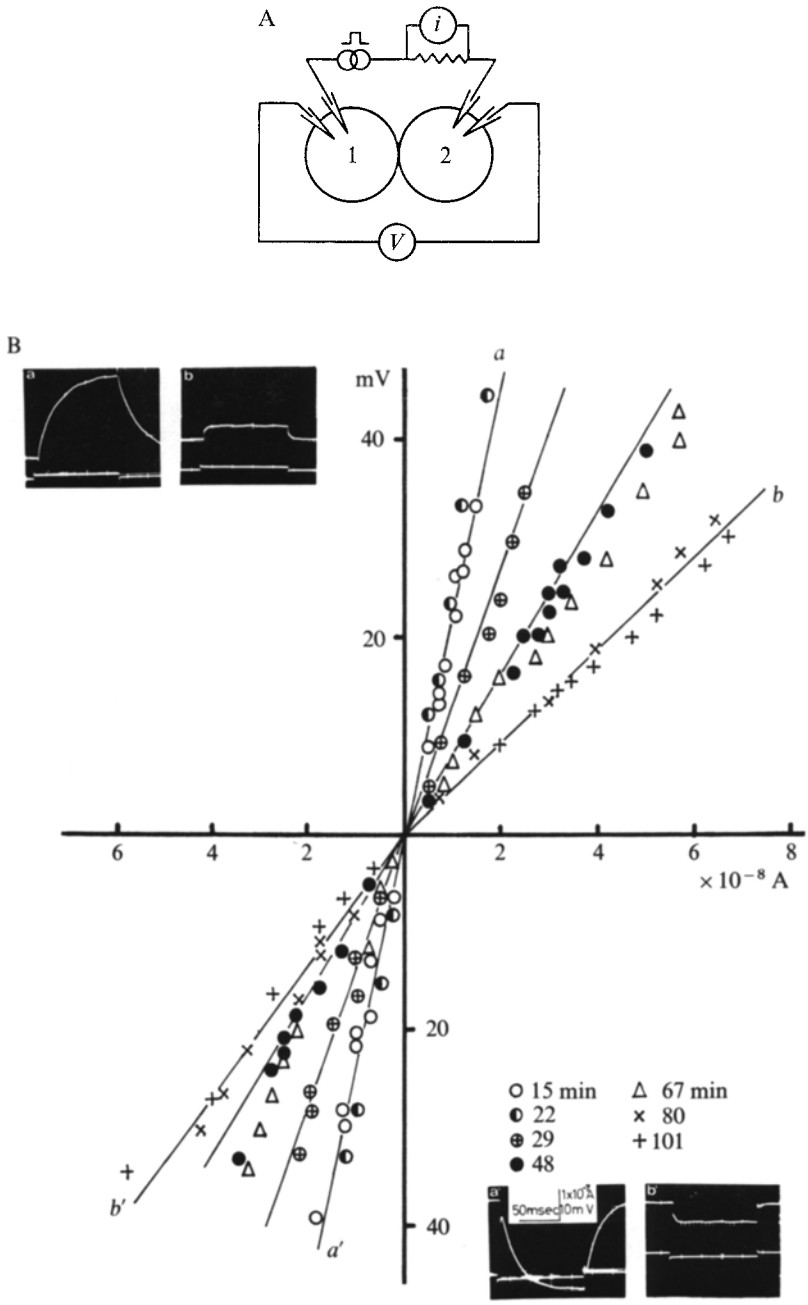

Fig. 6. Cell-to-cell resistance measurement. (*A*) Electrode arrangement. Current (i) is passed between the interiors of cells *1* and *2*, and the resulting voltage (V) is measured between the two cell interiors. (*B*) V *vs.* i curves. The curves were determined at different times after cell contact according to time schedule below. Outward current, right. The slope of the $b-b'$ curve approximates the junctional membrane resistance $2r_c$. *Insets.* Sample oscilloscope records of i (1.3×10^{-8} A) and V. Outward current upward

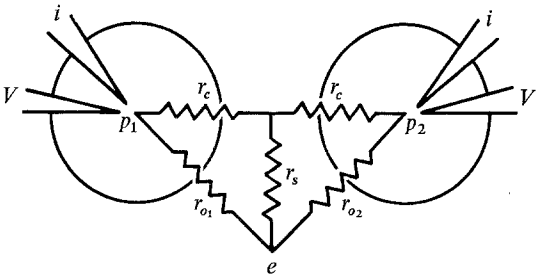

Fig. 7. Equivalent circuit of a coupling cell pair in a cell-to-cell resistance measurement. Notation as in Fig. 3. The *i*- and *V*-circuits are isolated from each other and from the external medium (*e*). The cell-to-cell resistance is the effective resistance between p_1 and p_2 due to all the pathways linking them

Furthermore, since the nonjunctional membrane resistance can be accurately determined from the slopes of the current-voltage curves (Fig. 9), it is clear that one can estimate specific resistance of nonjunctional membrane rather precisely. The mean specific resistance, R_o, obtained on a total of 56 cells (including those of Table 1) was 17.4 ± 6 (10^3 Ω cm^2), of the same order as calculated before (Ito & Loewenstein, 1969). This resistance value is in line with estimates for nonjunctional membrane in a variety of electrically excitable and inexcitable cells (for reviews *see* Eccles, 1953; Loewenstein, 1966).

The second point makes it clear that the area of junctional membrane in the fully joined cells is very much smaller than that of nonjunctional membrane. (In many other cell systems, this is evident even from light microscopy. However, in the present system, the region of cell "contact" apparent by light microscopy is unusually large.) Thus, the finding of resistance values of the same order for junctional ($2r_c$) and nonjunctional membranes (r_o) (Table 1) points up again the relatively low specific resistance of junctional membrane.

We do not have the exhaustive statistical data necessary for estimating the contact area between fully joined cells on the basis of electron-micrographs. But we can estimate an upper limit for this area in partly separated cells in experiments *Type 3* (*see* pp. 315–316 of paper I in this series) where the only visible coupling connection consisted of a few "*A*"-strands of known diameter. In three Type-3 experiments, the degree of coupling (V_2/V_1) mediated by some 3 or 4 *A*-strands, of 1-μ diameter, was nearly equal to that when initially the cells had been fully joined. Hence, the upper limit of junctional membrane area here was 10^{-8} cm^2, 5 orders of magnitude less than the nonjunctional membrane area.

From this and from the "steady-level" r_c values determined by the basic measurement, which were all in the range of 1–2 (10^6 Ω), we obtain an upper

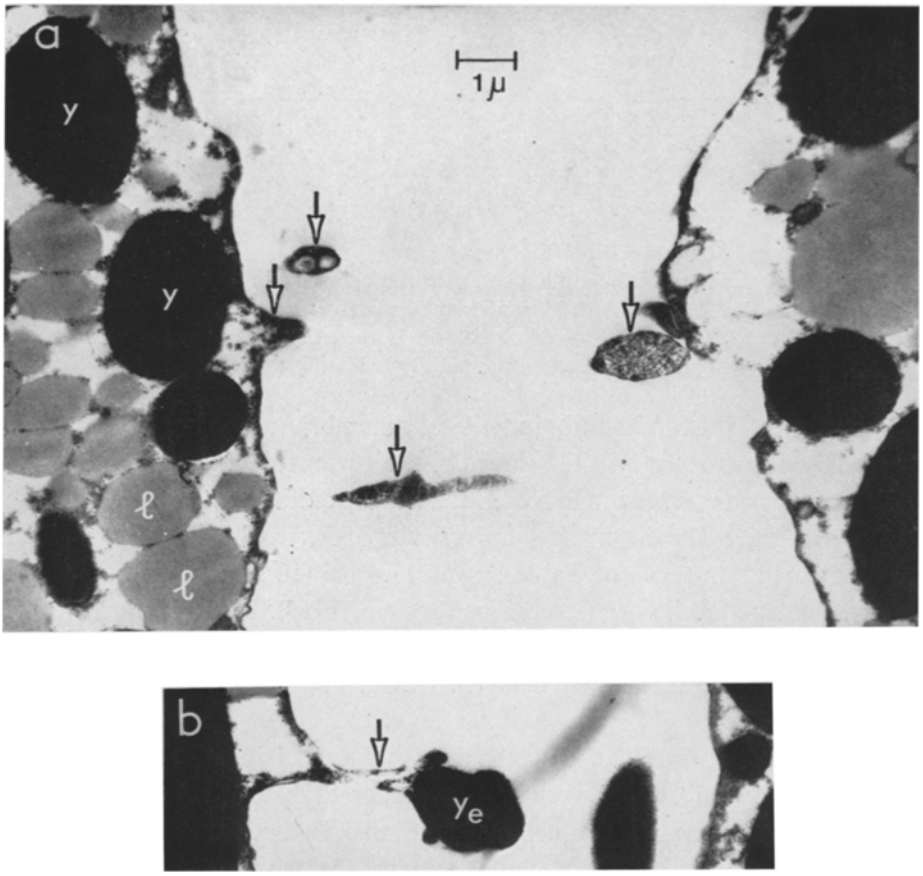

Fig. 8. Electron-micrographs of cell junction. The two cells had been micromanipulated into contact *(random imposed contact)* and fixed 60 min thereafter. (*a*) shows a transection of a region where the membranes of the two cells were generally >8 μ apart. The intercellular space is seen bridged here by a cell process (arrows) of about 0.3–0.4 μ diameter, presumably a motile protuberance (*see* paper I, Figs. 3 and 4). In (*b*) such a cell process is seen in contact with an extracellular yolk granule (y_e) (the bottom of the dish in which the cell junction was assembled was covered with yolk). *y* and *l* are, respectively, intracellular yolk and lipid granules. (*c*) and (*d*) show a region where the distance between the two membranes was generally <1 μ. Here three membrane spots are seen in close contact. One spot has a width of nearly 1 μ in this transection; the other two, 0.2–0.3 μ (unextended *A*- and *B*-strands?). *c* and *d* are pictures of the same transection

limit for the specific resistance of junctional membrane of the order of 10^{-2} Ω cm^2. The value is comparable to the earlier estimate of 10^{-2}–10^{-1} Ω cm^2 for this junction, based on less precise measurement of junctional membrane resistance (Ito & Loewenstein, 1969); and falls within the resis-

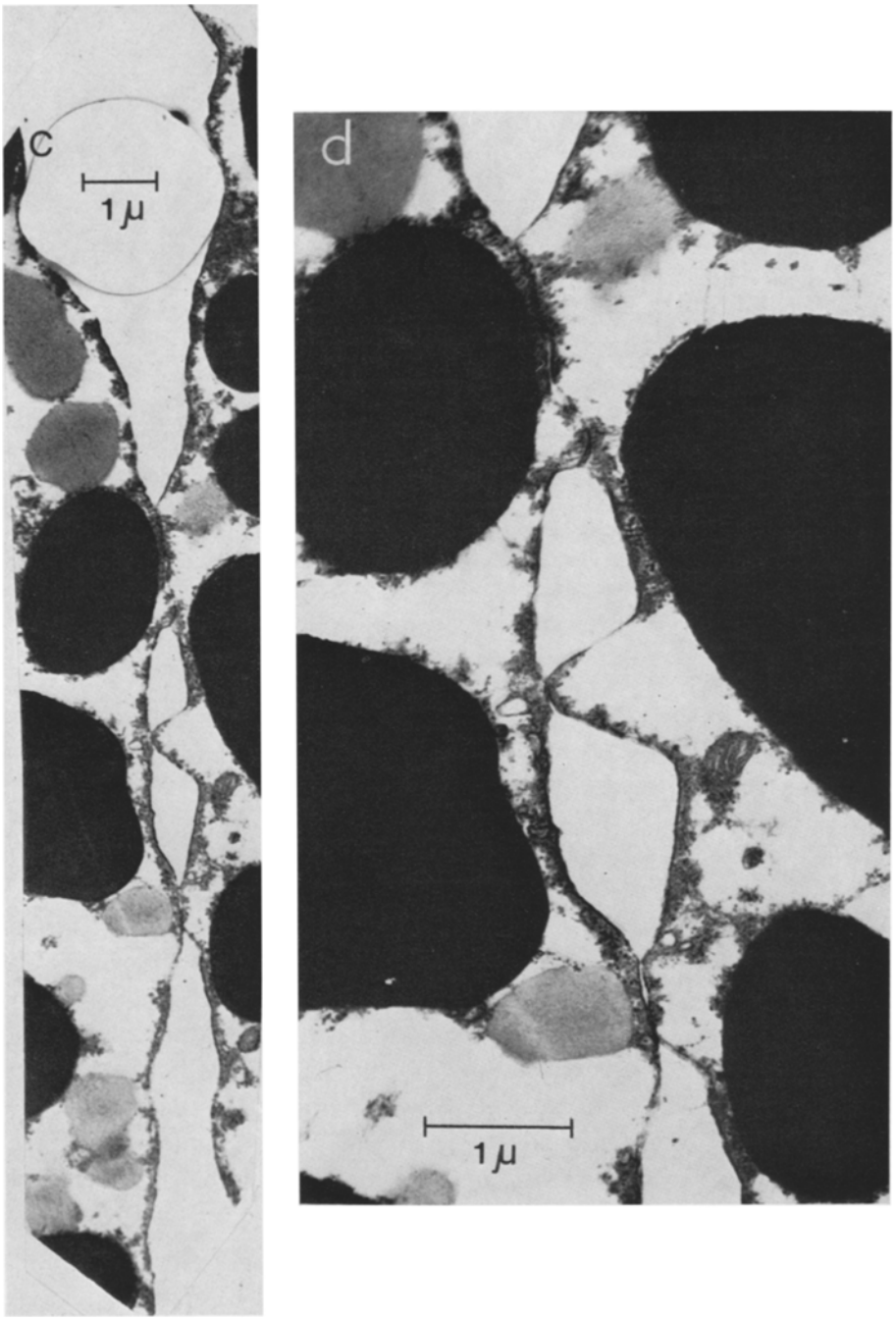

Fig. 8c and d

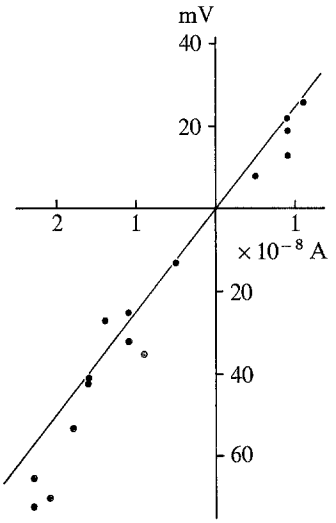

Fig. 9. A membrane current-membrane voltage curve, as used for the determination of nonjunctional membrane resistance r_o. *Abscissa:* outward (right) and inward current passed through membrane of a fully separate cell. *Ordinate:* the resulting voltage drops across the membrane. Least-square slope is 2.3 MΩ

tance range estimated for a variety of coupling cell types (Loewenstein *et al.*, 1965) (*compare also* with Bennett, 1966; Furshpan & Potter, 1968; Weidman, 1969; van Venrooij *et al.*, 1974).

Discussion

Junctional Conductance. The present results show that the establishment of coupling at a membrane junction is a progressive event: both the junctional conductance and the junctional insulation resistance increase gradually in the course of junction formation. In earlier work, the coupling ratio V_2/V_1 had been found to increase progressively during junction development (Loewenstein, 1967; Ito & Loewenstein, 1969). However, this did not necessarily show, of course, that junctional conductance increases. The coupling ratio is an experimentally convenient index, but it is a complex parameter that depends on junctional membrane resistance as well as on nonjunctional membrane resistance and junctional insulation resistance. The dependence is given by

$$\frac{V_1}{V_2}=1+\frac{2r_c}{r_{o_2}}+\frac{r_c}{r_s}\left(1+\frac{r_c}{r_{o_2}}\right)$$

(Loewenstein & Kanno, 1964). Thus, to infer changes of junctional membrane resistance $2r_c$ from observed changes in V_2/V_1, one needs information

on r_o and r_s, as we have obtained here for the first time, or equivalent information in terms of input resistance (Loewenstein, Nakas & Socolar, 1967).

The increase in junctional membrane conductance during coupling development means either (i) a gradual increase in specific conductance, that is, a gradual increase in conductance in a constant junctional area; or (ii) a gradual increase in area of junctional membrane of constant specific conductance; or (iii) an increase in both. In terms of the junctional model (Loewenstein, 1966), the simple interpretation is (ii). In this model (Fig. 1), the membrane junction is made of units *(junctional units)*, each complete with its junctional insulation (S), and a set of junctional membrane elements which, in the light of the present measurements (Table 1), would each have a specific conductance of 10^2 mho/cm^2. Thus, the measured increase in junctional conductance would reflect an increase in the number of functional junctional units. In other words, *coupling develops by addition of junctional units.*

Junctional Insulation. We will now attempt to interpret also the results of the determinations of junctional insulation resistance r_s in terms of this model. Characteristically, r_s first rises and then declines to a "steady" level during the coupling process (Figs. 4 and 5). If the junctional insulation resistance at each junctional unit, that is, the unit-r_s developed in an all-or-none fashion, the model would predict a step increase (as the first unit forms) followed by a gradual decline in (total) r_s, as the number of junctional units increases during junction formation. The results of Figs. 4 and 5 may be accommodated if the unit-r_s increases progressively during the coupling process. In this light, the rising phase in (total) r_s would reflect the dominance of the increasing value of unit-r_s over the effect of growing numbers of units in parallel; and the falling phase, the shift in dominance.

The foregoing interpretation presupposes that the observed resistance r_s is inherent principally in the structure of the S elements of the junctional units. But a significant r_s component may conceivably be associated with the convolution and constriction of leakage pathways between junctional units through the extracellular space (f, Fig. 1), constraints that would multiply as more and more units are formed. In this case, even an all-or-none mode of unit-r_s development would be possible; the rise of (total) r_s could then represent dominance of the increasing constraints over increasing leakage contributions due to growing numbers of S elements.

Structural Correlates. We have no electron-microscopic information on the junction of the present cell system to ponder the foregoing notions that

coupling develops by accretion of *junctional units*; and, in general, there is as yet little information about the structural correlates of coupling development. However, what little is known for other cell systems seems at least compatible with such a notion, if we may assume that the membrane particles, which in freeze-fracture electron-microscopy are seen forming arrays on the two adjoining membranes of the "gap" and the "septate junction" (reviews by McNutt & Weinstein, 1973; Satir & Gilula, 1973) contain or are identical with the halves of the *junctional units*. Gilula's (1971, 1973) work, the first to examine the formation of a junction by freeze-fracture electron-microscopy, indicates that the membrane particle array in the "septate junction" between sea urchin embryo cells is assembled progressively; the number of particles and their grouping increase with development. Johnson and Preuss (1973) report that the number of membrane particles in the "gap junction" forming between certain fibroblasts cultured from Novikoff's hepatoma, increases with time and that the first clusters of particles appear within 5 min of cell aggregation, at about the time coupling between these cells becomes detectable (Hammer, Epstein & Sheridan, 1973).

As to the structural correlates of the components of the *junctional unit*, the channelled membrane elements *C* and the junctional insulation *S*, there are presently several possibilities. A simple possibility is that the *C* elements reside in the hydrophilic regions of the membrane particles and that the *S* insulation is provided by the hydrophobic regions of the particles and by the junctions of these regions between the members of each pair of adjoining particles (*see* Figure on p. 114 of Loewenstein, 1974). This is plausible, because X-ray diffraction studies indicate that the particles in the adjoining membranes of the gap junction are aligned (Goodenough and Caspar, *personal communication*), and is in line with present general concepts of membrane channels (*cf.* Singer, 1973).

We thank Dr. S. J. Socolar for helpful discussion, Dr. M. Goto for valuable assistance and Prof. Miyawaki for kindly providing us with the electron-micrographs.

This work was supported by grants 854175 and 954189 from the Ministry of Education of Japan, by U.S. Public Health Service research grant No. CA 14464, and National Science Foundation grant No. GB 36763X1.

References

Bennett, M. V. L. 1966. Physiology of electrotonic junctions. *Ann. N.Y. Acad. Sci.* **137**:509

Eccles, J. C. 1953. The Neurophysiological Basis of Mind. Clarendon Press, London, England

Furshpan, E. J., Potter, D. D. 1968. Low resistance junctions between cells in embryos and tissue culture. *Curr. Top. Devel. Biol.* **3**:95

Gilula, N. B. 1971. Studies on the Septate Junction. Ph. D. Thesis. University of California, Berkeley

Gilula, N. B. 1973. Development of cell junctions. *Amer. Zool.* **13**:1109

Hammer, M., Epstein, M., Sheridan, J. 1973. Gap junction formation in a reaggregating system. *J. Cell Biol. (Abstr)* **59**:130a

Ito, S., Loewenstein, W. R. 1969. Ionic communication between early embryonic cells. *Devel. Biol.* **19**:228

Ito, S., Sato, E., Loewenstein, W. R. 1974. Studies on the formation of a permeable cell membrane junction. I. Coupling under various conditions of membrane contact. Effects of colchicine, cytochalasin B, dinitrophenol. *J. Membrane Biol.* **19**:305

Johnson, R., Preuss, D. 1973. Gap junction formation in a reaggregating system: An ultrastructural study. *J. Cell Biol. (Abstr)* **59**:158a

Loewenstein, W. R. 1966. Permeability of membrane junctions. *Ann. N.Y. Acad. Sci.* **137**:441

Loewenstein, W. R. 1967. On the genesis of cellular communication. *Devel. Biol.* **15**:503

Loewenstein, W. R. 1974. Cellular communication by permeable membrane junctions. *Hosp. Prac. (Membrane Series)* **9**:113

Loewenstein, W. R., Kanno, Y. 1964. Studies on an epithelial (gland) cell junction. I. Modifications of surface membrane permeability. *J. Cell Biol.* **22**:565

Loewenstein, W. R., Nakas, M., Socolar, S. J. 1967. Junctional membrane uncoupling. Permeability transformations at a cell membrane junction. *J. Gen. Physiol.* **50**:1865

Loewenstein, W. R., Socolar, S. J., Higashino, S., Kanno, Y., Davidson, N. 1965. Intercellular communication: Renal, urinary bladder, sensory, and salivary gland cells. *Science* **149**:295

MacNutt, N., Weinstein, R. S. 1973. Membrane ultrastructure at mammalian intercellular junction. *Prog. Biophys. Mol. Biol.* **26**:45

Satir, P., Gilula, N. B. 1973. The fine structure of membranes and intercellular communication in insects. *Annu. Rev. Entomol.* **18**:143

Singer, S. J. 1973. Architecture and topography of biologic membranes. *Hosp. Prac. (Membrane Series)* **8**:81

Venrooij, G. E. P. M. van, Hax, W. M. A., Dantzig, G. F. van, Prijs, V., Denier van der Gon, J. J. 1974. Model approaches for the evaluation of electrical cell coupling in the salivary gland of the larva of *Drosophila hydei*. The influence of lysolecithin on the electrical coupling. *J. Membrane Biol.* **19**:229

Weidmann, S. 1969. Electrical coupling between myocardial cells. *Prog. Brain Res.* **31**:276